

**Particle
concentration as the
indicator of formation
mechanism**

J. Lauros et al.

Particle concentration and flux dynamics in the atmospheric boundary layer as the indicator of formation mechanism

J. Lauros¹, A. Sogachev², S. Smolander¹, H. Vuollekoski¹, S.-L. Sihto¹,
I. Mammarella¹, L. Laakso³, Ü. Rannik¹, and M. Boy¹

¹Department of Physics, University of Helsinki, Finland

²Wind Energy Division, Risø National Laboratory for Sustainable Energy, Technical University of Denmark, Roskilde, Denmark

³School of Physical and Chemical Sciences, North-West University, Potchefstroom, South Africa

Received: 11 July 2010 – Accepted: 13 August 2010 – Published: 24 August 2010

Correspondence to: J. Lauros (johanna.lauros@alumni.helsinki.fi)

Published by Copernicus Publications on behalf of the European Geosciences Union.

Title Page

Abstract

Introduction

Conclusions

References

Tables

Figures

⏪

⏩

◀

▶

Back

Close

Full Screen / Esc

Printer-friendly Version

Interactive Discussion

Abstract

We carried out column model simulations to study particle fluxes and deposition and to evaluate different particle formation mechanisms at a boreal forest site in Finland. We show that kinetic nucleation of sulphuric acid cannot be responsible for new particle formation alone as the vertical profile of particle number distribution does not correspond to observations. Instead organic induced nucleation leads to good agreement confirming the relevance of the aerosol formation mechanism including organic compounds emitted by biosphere.

Simulation of aerosol concentration inside the atmospheric boundary layer during nucleation days shows highly dynamical picture, where particle formation is coupled with chemistry and turbulent transport. We have demonstrated suitability of our turbulent mixing scheme in reproducing most important characteristics of particle dynamics inside the atmospheric boundary layer. Deposition and particle flux simulations show that deposition affects noticeably only the smallest particles at the lowest part of the atmospheric boundary layer.

1 Introduction

The formation of new particles remains one of the greatest challenges in atmospheric aerosols research. In spite of decades of intensive research, no one-for-all solution has been presented. As meteorological conditions and the composition of vapours vary spatially in the atmosphere, several formation mechanisms have been proposed.

Among the most cited mechanisms are the binary (Vehkamäki et al., 2002) and ternary (Napari et al., 2002) nucleation. However, they predict the existence of 4–10 sulphuric acid molecules in the critical cluster, whereas many experimental studies have found a linear to quadratic relationship between the new particle formation rate and sulphuric acid concentration (Weber et al., 1996; Kulmala et al., 2006; Sihto et al., 2006; Riipinen et al., 2007; Kuang et al., 2008; Sihto et al., 2009; Vuollekoski et al., 2010). In accordance with these recent findings, semi-empirical nucleation mecha-

Particle concentration as the indicator of formation mechanism

J. Lauros et al.

Title Page

Abstract

Introduction

Conclusions

References

Tables

Figures

⏪

⏩

◀

▶

Back

Close

Full Screen / Esc

Printer-friendly Version

Interactive Discussion



nisms have been presented, such as the activation of pre-existing clusters (Hoppel et al., 1994; Kulmala et al., 2006).

Lately, the role of organics in new particle formation has gained more and more interest. Some studies have found that the growth rate calculated from the concentration of sulphuric acid is not enough to explain the growth of ultrafine particles (Weber et al., 1997; Birmili et al., 2003; Boy et al., 2005). This suggests the condensation of an additional, low-volatile vapour. Recently, the participation of such vapour in the nucleation step itself has been studied (e.g., Bonn et al., 2009; Paasonen et al., 2010; Vuollekoski et al., 2010).

In the meteorological sense, the mixing of atmospheric constituents – in particular aerosol particles – is challenging. The simplest, first order mixing parametrisations (see e.g., Stull, 1989), the so called gradient transport theory or K-theory, have not succeeded to present turbulent mixing in all atmospheric layers and conditions, so higher order models have been developed and utilised also in aerosol studies (e.g., Hellmuth, 2006a,b,c,d). Some parametrisations add a separate nonlocal counter-gradient transport term to the flux equation (e.g., Noh et al., 2003). The idea is that the transport should depend strongly on the surface gradient, instead of the local gradient of the studied quantity. This approach may be convenient when modelling heat flux and other similarly behaving quantities. In the case of aerosol flux, the surface gradient of particle concentration does not describe the strength of the mixing in the same manner as it does for e.g. temperature gradient. The results may be opposite to intended, when particle concentration increases upwards and the added term leads to weaker mixing than the parametrisation without the counter-gradient term.

It would be easy to assume that if a model includes more complex structures of turbulence, this improves the results significantly. However, complex parametrisations may be sensitive to particular parameter values, which may be unreliable. For this study, we have chosen a one-and-half order parametrisation (Boy et al., 2010) which presents mixing better than first order models and is more proper for aerosol flux than the counter-gradient models mentioned above.

Particle concentration as the indicator of formation mechanism

J. Lauros et al.

Title Page

Abstract

Introduction

Conclusions

References

Tables

Figures



Back

Close

Full Screen / Esc

Printer-friendly Version

Interactive Discussion



Particle concentration as the indicator of formation mechanism

J. Lauros et al.

[Title Page](#)[Abstract](#)[Introduction](#)[Conclusions](#)[References](#)[Tables](#)[Figures](#)[⏪](#)[⏩](#)[◀](#)[▶](#)[Back](#)[Close](#)[Full Screen / Esc](#)[Printer-friendly Version](#)[Interactive Discussion](#)

In this article, we aim to increase knowledge in particle formation mechanisms utilising fluxes and vertical distribution of particles in the atmospheric boundary layer (ABL). As we are interested in particle formation especially in the lowest part of the atmosphere, we concentrate on testing theories of organic nucleation mechanisms and compare the results with the conventional kinetic nucleation theory. As ion-induced nucleation is typically in Hyytiälä of minor importance, on average ~10% of the total nucleation (Manninen et al., 2009; Gagné et al., 2008; Laakso et al., 2004), we investigate in this study neutral pathways. In addition, we study the effect of turbulent mixing, dilution and deposition on particle formation, and evaluate the adequacy of the developed model in aerosol studies.

2 Measurements

The measurements were carried out at the SMEAR II station in Southern Finland. A detailed description of the station and instrumentation is given by Kulmala et al. (2001) and in <http://www.atm.helsinki.fi/SMEAR/>. The particle size distributions between 3–1000 nm were measured by a twin differential mobility particle sizer (TDMPMS) inside forest. In addition, vertical profiles of meteorological variables (temperature, humidity) and number concentration of particles (>10 nm in diameter, measured by two condensation particle counters) were measured on hot-air balloon flights (Laakso et al., 2007).

3 Model

The 1-dimensional column model of ABL used in this study is a further development of the model MALTE (Model to predict new Aerosol formation in the Lower TropospherE) which is described in detail by Boy et al. (2006, 2008). The model reproduces the diurnal variation of boundary layer meteorology, chemistry, emissions and particle formation. We have improved the meteorology scheme (turbulence, radiation), as compared

to MALTE, by utilising a one-dimensional version of the model SCADIS (Sogachev et al., 2002; Sogachev and Panferov, 2006; Sogachev, 2009). In our simulations the model consists of 52 layers, of which 18 are inside canopy in the lowest 15 m.

3.1 Meteorological scheme

We replaced the original turbulence scheme in MALTE with that of SCADIS to get more reliable results considering vertical turbulent (heat, vapour and aerosol) fluxes. The fluxes are expressed as a product of turbulent diffusion coefficient and gradient of a mean quantity. Atmospheric boundary layer model SCADIS includes originally a set of movement equations, the continuity equation, equations for moisture and heat transport, and also it is able to implement transport equation of passive tracer of interest. The time-marching method is used to solve the nonlinear two-point boundary-value problems. SCADIS applies one-and-half-order closure scheme, when the equation for turbulent kinetic energy and the equation of a supplementary characteristic (in SCADIS that is specific dissipation) have to be solved to estimate the diffusion coefficient. Considering the vegetation as multi-layer medium and implementing parametrisations for radiation transfer, drag forces on leaves and stomatal conductance, SCADIS properly describes the exchange between the vegetative canopy and atmosphere. In our simulations observations of direct and diffuse solar radiation above canopy were utilised as border values for radiation transfer scheme.

3.2 Chemistry and emissions

The model presents time-dependent concentrations of 45 chemical species which result from 112 reactions. Sulphuric acid and reaction products of organic vapours (monoterpenes) are the most essential simulated vapours in our study as these take part into particle formation.

KPP – the Kinetic PreProcessor (Damian, 2002; Sandu and Sander, 2006) is now used in MALTE to translate the reaction equations (for details see Boy et al., 2006)

Particle concentration as the indicator of formation mechanism

J. Lauros et al.

Title Page

Abstract

Introduction

Conclusions

References

Tables

Figures

⏪

⏩

◀

▶

Back

Close

Full Screen / Esc

Printer-friendly Version

Interactive Discussion



Particle concentration as the indicator of formation mechanism

J. Lauros et al.

[Title Page](#)[Abstract](#)[Introduction](#)[Conclusions](#)[References](#)[Tables](#)[Figures](#)[⏪](#)[⏩](#)[◀](#)[▶](#)[Back](#)[Close](#)[Full Screen / Esc](#)[Printer-friendly Version](#)[Interactive Discussion](#)

into Fortran 90 code that performs the time integration of the kinetic system. Of the several numerical solvers for systems of differential equations available in KPP, we used the LSODE solver (Radhakrishnan and Hindmarsh, 1993; Sandu et al., 1997). The KPP-produced Fortran code is then called from main MALTE code. Some minimal changes to the KPP-produced code were performed. The chemistry and meteorology are combined in a typical split-operator approach. Meteorology, including atmospheric mixing of the chemical species, is simulated with a 10 s time step and after each 6 steps chemistry, separately for each atmosphere layer, is simulated for 60 s. Thus, the changes in the chemical concentrations after the chemistry step would appear instantaneous from the meteorology model point of view.

The emissions of monoterpenes from the canopy are calculated with MEGAN (Model of Emissions of Gases and Aerosols from Nature), which is described by Guenther et al. (2006). The emission rates depend on leaf temperature and available solar radiation on sun and shade calculated separately for every model level.

3.3 Particle formation and growth

The aerosol dynamic processes are simulated with the multicomponent aerosol dynamics model UHMA (Korhonen et al., 2004). The scheme includes representation of nucleation mechanisms, activation of nano-size clusters following nano-Köhler theory (Kulmala et al., 2004), condensation and coagulation (see also Boy et al., 2006). We consider different formation paths for new particles. The first mechanism is called kinetic type nucleation and was first proposed by McMurry and Friedlander (1979). In kinetic nucleation, critical clusters are formed by collisions of sulphuric acid molecules or other molecules containing sulphuric acid, e.g. ammonium bisulphate molecules. The upper limit for kinetic nucleation, the kinetic limit, is set by the collision rate of molecules given by the kinetic theory of gases. Here we let the collision frequency function be a free parameter and calculate nucleation rate as:

$$J = K \times [\text{H}_2\text{SO}_4]^2 \quad (1)$$

The coefficient K in our study was set to $5 \times 10^{-13} \text{ cm}^3 \text{ s}^{-1}$ based on best fit after comparison of simulated and observed particle concentrations on studied time period. This kinetic coefficient K contains the details of the nucleation process, specifically the probability that a collision of two sulphuric acid containing molecules results in the formation of a stable critical cluster.

The second nucleation mechanism, organic nucleation rate, is presented in sense of kinetic nucleation with the assumption that new particles are formed through collisions between sulphuric acid molecules and molecules which are reaction products of organic vapours (MoRP, monoterpenes reaction products). So the formation rate depends on the concentration of vapours (H_2SO_4 , MoRP) and molecular collision probability:

$$J = P\nu[\text{H}_2\text{SO}_4][\text{MoRP}]. \quad (2)$$

Here ν is the collision rate and the constant P describes the probability that a collision leads to new particle formation. Similarly as above we defined value of P based on best fit for studied formation paths and used a value of $1-2 \times 10^{-4} \text{ cm}^3$ depending on organic reaction products which are participating nucleation. As the formation rate depends on organic vapour concentration, the expected maximum of particle formation rate is located at the surface close to organic vapour sources and the rate decreases upwards.

Nucleation is followed by growth according to nano-Köhler theory having sulphuric acid and reaction products of organics with OH as condensing vapour. After this water, sulphuric acid and reaction products of organics with OH, NO_3 and O_3 participate in the growth of particles.

3.4 Particle deposition to the canopy

In the earlier model version deposition to canopy was presented by a bulk parametrization as the model had only one level describing the removal effect. As the new model

Particle concentration as the indicator of formation mechanism

J. Lauros et al.

Title Page

Abstract

Introduction

Conclusions

References

Tables

Figures

⏪

⏩

◀

▶

Back

Close

Full Screen / Esc

Printer-friendly Version

Interactive Discussion



version has several levels inside canopy a more sophisticated deposition parametrisation is possible.

We follow Petroff et al. (2008) to parametrise deposition to needles. Vegetation collection rate r_k (s^{-1}) due to process k in a layer,

$$r_k = af_k v_k \quad (3)$$

depends on surface area of needles a and the elemental collection velocity v_k . The factor f_k describes the ratio of the averaged and the elemental collection velocity and depends on angular and size distribution of needles in a layer. The vegetation removal rate R_k ($\text{cm}^{-3} \text{s}^{-1}$) is a product of the vegetation collection rate and particle concentration:

$$R_k = r_k \times C \quad (4)$$

We assume that the total deposition is a sum of individual processes and parametrised separately deposition due to Brownian diffusion, gravitational settling, interception and inertial impaction. The two latter processes depend stronger on wind velocity than Brownian diffusion. The influence of interception exceeds effect of Brownian diffusion already at low wind velocities when particles are larger than 100 nm (see Petroff et al., 2008) and for 25 nm particles interception begins to dominate if wind speed exceeds 4 m s^{-1} . For interception and impaction calculation we assume that the angle distribution of needles in the space and size distribution of diameter are uniform.

Brownian diffusion due to thermal motion is most important for small particles. The elemental collection velocity due to Brownian diffusion is defined for needles as (Petroff et al., 2008)

$$v_B = \frac{ShD_B}{d_n} \quad (5)$$

where D_B ($\text{m}^2 \text{s}^{-1}$) is the diffusivity of a particle and the mean diameter of needles d_n was set to 1 mm. Sherwood number is defined as $Sh = C_B Sc^{1/3} Re^{n_B}$ where Re

Particle concentration as the indicator of formation mechanism

J. Lauros et al.

[Title Page](#)[Abstract](#)[Introduction](#)[Conclusions](#)[References](#)[Tables](#)[Figures](#)[⏪](#)[⏩](#)[◀](#)[▶](#)[Back](#)[Close](#)[Full Screen / Esc](#)[Printer-friendly Version](#)[Interactive Discussion](#)

is Reynolds number and C_B and n_B are adjusted parameters which depend on flow regime through Re .

Deposition velocity is defined as

$$V_d(z) = -\frac{F_t(z)}{C(z)} + W_s \quad (6)$$

5 where F_t is turbulent flux and W_s settling velocity. At the surface we calculate deposition velocity as Petroff et al. (2008):

$$V_{dg} = 3\sqrt{3}/(29\pi)Sc^{-2/3}u_* + W_s \quad (7)$$

where Sc is Schmidt number and u_* friction velocity (in this study at the first model level above the surface). Settling velocity is calculated as described by Rannik et al. (2003).

10 For details of parametrisations, see Petroff et al. (2008).

4 Results

We simulated new particle formation on 12–14 March 2006. On these event days hot-air balloon flights were carried out (Laakso et al., 2007). The initial gas concentrations of most species, especially the organic reaction products, were set to zero during the night at the start of the model run. For several other gases like CO, SO₂, NO, NO_x and ozone, measurements from the SMEAR II station were used. Sulphuric acid was calculated from oxidation of observed SO₂ and organic vapours originated from calculated canopy emissions. The initial particle distribution corresponded surface observations in the ABL (below 300 m) and was set to 0.2 of the observed concentration at higher altitudes in the free troposphere.

4.1 Evaluation with meteorology

Meteorological conditions were dominated by a high pressure which centre moved from Scandinavian Peninsula to Finland. The simulated mixing height, defined in the

20013

Particle concentration as the indicator of formation mechanism

J. Lauros et al.

Title Page

Abstract

Introduction

Conclusions

References

Tables

Figures

⏪

⏩

◀

▶

Back

Close

Full Screen / Esc

Printer-friendly Version

Interactive Discussion



simulations as an altitude where Richardson number exceeds 0.25, is typical for spring time in Finland and the early growth was consistent with SODAR measurements at SMEAR II station (Fig. 1a). However, the simulated humidity profiles show underestimation in concentration in the free troposphere on afternoon. As the source of humidity is at the surface, this together with the temperature profiles indicate underestimation in mixing strength especially above the ABL (Fig. 1b). The weak mixing affects vapour concentrations leading to strong concentration gradient between the ABL and the free troposphere which will be discussed more in details in Sects. 4.2.2 and 4.3.

4.2 Particle formation paths

4.2.1 Kinetic nucleation

Kinetic nucleation (Eq. 1) represents the observed particle formation events at the surface with the limitation that on the selected days change of air masses by horizontal advection most likely prevented the appearance of clear “banana-plots” compared to the model (Fig. 2a and b). However, even if we are able to reproduce surface observations, the simulated vertical particle profiles do not correspond the observed ones at all. The kinetic nucleation prefers new particle formation in the free troposphere where pre-existing particle concentrations are low. The nucleation rate follows diurnal variation of sulphuric acid but the number concentration of aerosols increases constantly above the ABL due to low sink and the higher sulphuric acid concentration above. The observed profiles for particles greater than 10 nm in diameter refers to particle formation inside the ABL as the number concentration decreases notably just above the ABL (Fig. 3). Based on our simulations and earlier studies (Makkonen et al., 2009), kinetic nucleation cannot be the prime particle formation mechanism in the lower troposphere at the boreal forest site.

Particle concentration as the indicator of formation mechanism

J. Lauros et al.

Title Page

Abstract

Introduction

Conclusions

References

Tables

Figures

⏪

⏩

◀

▶

Back

Close

Full Screen / Esc

Printer-friendly Version

Interactive Discussion



4.2.2 Organic-induced formation

We have simulated different paths for new particle formation and tested organic components which participated in nucleation and nano-Köhler growth. When nucleation rate depends on the reaction products of organic molecules (monoterpenes) with O₃ particles are formed even in the night as the concentration of reaction products does not decrease significantly. This leads to presence of smallest particles in the night in simulation whereas 3–6 nm particles are not observed similarly during night (Fig. 2c). Decreasing P in Eq. (2) does not help as the formation rate decreases similarly at observed event time and the diurnal variation in concentration of reaction products of monoterpenes with O₃ is too small. The result is improved if nucleation rate depends on reactions products of monoterpenes with OH instead of O₃ as clear events are predicted (Fig. 2d). In the presented simulations (Fig. 2c and d) we have assumed that 5% of organic reaction products are able to condense on freshly nucleated particles. The value has led to good agreement with observations in earlier (Boy et al., 2006) and present study.

Simulated new particle formation rate decreases upwards as organic gas concentration decreases. This leads to similar number of particles (>10 nm in diameter) as observed (Fig. 3): concentration is constant inside the ABL due to strong mixing but decreases substantially above the ABL. The particle concentration is slightly overestimated in the ABL but the concentration corresponds very well to the observations in the residual layer and further up to 500 m. Between 500–1200 m the simulated concentrations follow the initial model concentrations instead of the observations. As the simulated concentration of smallest particle is similarly very low at these altitudes, the underestimation of larger particles does not result from slow growth of particles. A reason can be too weak mixing and flow of 10–1000 nm particles from the ABL or lack of advection of particles in the free troposphere (different background aerosol distribution) that is not included in 1-D modelling. As the concentration of nucleating and condensing organic vapours is probably underestimated due to weak mixing just above the ABL,

Particle concentration as the indicator of formation mechanism

J. Lauros et al.

Title Page

Abstract

Introduction

Conclusions

References

Tables

Figures



Back

Close

Full Screen / Esc

Printer-friendly Version

Interactive Discussion



the underestimation of local particle formation is a plausible reason. Earlier observations approve that new particle formation is possible in the residual layer (Stratmann et al., 2003; Laakso et al., 2007).

In sense of mixing the situation is different in comparison to conventional kinetic nucleation, as the particle formation rate decreases upwards in the ABL similarly as concentration of reaction products of organics. Thereby the particle formation path is convenient to study mixing of particles, when most of the new particles are formed in the lower half of the ABL. In following simulations nucleation rate depends on reaction products of organics and OH.

4.3 Dilution due to entrainment and deposition

4.3.1 Entrainment and particle fluxes

Decrease in surface particle concentration has been recognised regularly in forenoons before a particle formation event occurs (Boy et al., 2004). The decrease has been explained by onset of mixing and flow of cleaner air from free troposphere to the surface. Our simulations show dilution at the surface following dilution at the top of the ABL (Fig. 4). Simulated dilution is stronger in the upper part of the ABL than at the surface. Dilution occurs after onset of new particle formation, and thus decreasing sink due to dilution of background aerosol concentration cannot activate particle formation in our simulations.

When the boundary layer grows and the mixing achieves upper cleaner air, this leads to concentration gradient and particle flux upwards toward lower concentrations (Fig. 5). Fluxes of larger particles (>25 nm) (Fig. 5c,d) is constantly upwards achieving maximum strength at the upper part of the ABL after noon.

The conditions for organic-induced particle formation and growth are most favourable at the surface which creates a vertical concentration difference and upward flux of smallest particles. The direction of smallest particles flux turns downwards after the ABL growth ends (Fig. 5a). The downward flux of particles requires downward

Particle concentration as the indicator of formation mechanism

J. Lauros et al.

Title Page

Abstract

Introduction

Conclusions

References

Tables

Figures



Back

Close

Full Screen / Esc

Printer-friendly Version

Interactive Discussion



Particle concentration as the indicator of formation mechanism

J. Lauros et al.

Title Page

Abstract

Introduction

Conclusions

References

Tables

Figures

⏪

⏩

◀

▶

Back

Close

Full Screen / Esc

Printer-friendly Version

Interactive Discussion

decreasing concentration which can result from removal of small particles near surface. The flux turns even if the deposition to canopy is ignored. Therefore the explanation is probably coagulation sink of small particles near surface as the concentration of larger particles is higher at the surface than at higher altitudes. The deposition, however, explains the constant downward flux of smallest particles near surface inside the canopy. Similarly as for 3–6 nm particles, 3–25 nm particle flux is downwards and opposite to larger particle flux during night and does not turn upwards until at noon when fresh-formed particles have achieved the size class. The flux in both the smallest size classes, 3–6 nm and 3–25 nm, turns upwards simultaneously as the lower limit of size classes is the same. On afternoon, the flux of 3–6 nm particles turns downwards before 3–25 nm particle flux. The growth of particles is favourable near surface and new particles achieve larger sizes later than smallest sizes. Due to favourable particle growth at the surface the vertical distribution of 3–25 nm particles evens out slower and the flux continues upwards longer than for the smallest studied size range.

The change of particle concentration depends on the gradient of turbulent fluxes and other terms related to aerosol dynamics:

$$\frac{dC}{dt} = -\frac{dF_t}{dz} + S_{ad}. \quad (8)$$

Here S_{ad} represents particle formation, sources and removal processes (deposition, coagulation, sinks). Under steady-state conditions the particle concentration does not change in the layer if the flux is spatially constant; as many particles are flowing in and out of the layer. We have calculated effect of fluxes on particle concentration from simulated particle fluxes (Fig. 6). Even if the particle flux is strong inside the ABL, it leads only to minor change in particle concentration of largest particles as gradient of particle flux is insignificant. The concentration of largest particles changes moderately and mainly just above the ABL where the strength of mixing changes strongly and the particle concentration gradient is large. Maximum effect on particle concentration due to mixing can be seen in smallest 3–6 nm particles in the ABL. The flux results from strong new particle formation in the ABL which leads to particle concentration gradient

between the ABL and free troposphere. The nighttime downward flux of 3–25 nm particles leads to decrease of particle concentration above the ABL and increase of concentration near the surface, respectively (Fig. 6b). However, the removal processes exceed the effect of nighttime flux and the particle concentration decreases at the surface (Fig. 4a).

4.3.2 Deposition to canopy

In addition to coagulation, turbulent mixing and entrainment to free troposphere, deposition to canopy removes particles in the ABL. The stronger turbulence is the stronger deposition is as especially interception strengthens.

The simulated wind velocity is 1–2 m s⁻¹ inside canopy and therefore Brownian diffusion is emphasised. Low wind velocity leads predominantly to removal of freshly nucleated and Aitken mode particles while Brownian diffusion does not affect similarly concentration of larger particles (Fig. 7). If wind velocity was significantly higher and interception stronger the removal rate of largest particles could exceed removal rate of Aitken mode particles. However, Brownian diffusion of smallest particles is so effective that these are removed fastest due to deposition regardless of wind velocity.

In canopy deposition removes smallest 3–6 nm particles up to 10 cm⁻³ s⁻¹ while the removal rate for 100–1000 nm particles is only up to 0.1 cm⁻³ s⁻¹ (Fig. 8). The diurnal variation in removal rate results from variation in particle concentration.

5 Conclusions

Our results point out the importance of mixing and a reliable mixing scheme in new particle formation studies. We succeeded to reproduce observed new particle formation events at the surface by applying kinetic and organic nucleation theory. The vertical profiles however showed that kinetic nucleation did not correspond the observed particle formation as the particle concentration became too high above the ABL. Instead

Particle concentration as the indicator of formation mechanism

J. Lauros et al.

Title Page

Abstract

Introduction

Conclusions

References

Tables

Figures

⏪

⏩

◀

▶

Back

Close

Full Screen / Esc

Printer-friendly Version

Interactive Discussion



Particle concentration as the indicator of formation mechanism

J. Lauros et al.

[Title Page](#)[Abstract](#)[Introduction](#)[Conclusions](#)[References](#)[Tables](#)[Figures](#)[⏪](#)[⏩](#)[◀](#)[▶](#)[Back](#)[Close](#)[Full Screen / Esc](#)[Printer-friendly Version](#)[Interactive Discussion](#)

organic-induced particle formation resulted in similar surface events and structure of vertical particle profile as the observations. This result allows to conclude that the organic-induced formation mechanism is responsible for particle formation at a Boreal forest site. Similar vertical profiles of particles during observed nucleation events have been observed at SMEAR II (Laakso et al., 2007; O'Dowd et al., 2009) and at other locations (e.g., Stratmann et al., 2003). Thus this mechanism could be an important path to atmospheric nucleation over forested areas and potentially also at other areas where emission of organic compounds occurs.

The underestimation of mixing led to overestimated gradient in vapour concentration at the top of the mixed layer. As the nucleation and condensing vapour concentration were probably underestimated, we were not able to reproduce particle formation processes above the ABL convincingly. The importance of reliable mixing scheme for top of the ABL and layers above the ABL is emphasised when particle formation is considered.

Petroff et al. (2008) showed that deposition of Aitken mode particles is mainly controlled by Brownian diffusion. The simulated wind velocity inside canopy was only up to few meters per second which decreased especially influence of interception of largest particles. Therefore deposition as particle sink inside forest affected mainly nucleation mode particles. The particle concentration and flux dynamics inside the ABL was mainly driven by particle formation, aerosol dynamical processes (growth to next size class) and atmospheric mixing. Particle deposition to forest affected mostly concentration of particles near surface but ignoring the deposition process did not change particle fluxes substantially. Therefore deposition had minor effect in comparison to particle dynamical processes and atmospheric mixing in our study. The conclusion applies to highly dynamical conditions of particle concentration and fluxes inside the ABL without implication to long-term significance of deposition mechanisms for particle removal from the atmosphere.

Acknowledgements. This work was supported by the Helsinki University Centre for Environment (HENVI), the Academy of Finland (project number: 1126009) and the Maj and Tor Nessling foundation (project number: 2009253). The financial support by the Academy of Finland Centre of Excellence program (project number: 1118615) is gratefully acknowledged.

5 References

Birmili, W., Berresheim, H., Plass-Dülmer, C., Elste, T., Gilge, S., Wiedensohler, A., and Uhrner, U.: The Hohenpeissenberg aerosol formation experiment (HAFEX): a long-term study including size-resolved aerosol, H₂SO₄, OH, and monoterpenes measurements, *Atmos. Chem. Phys.*, 3, 361–376, doi:10.5194/acp-3-361-2003, 2003. 20007

Bonn, B., Boy, M., Kulmala, M., Groth, A., Trawny, K., Borchert, S., and Jacobi, S.: A new parametrization for ambient particle formation over coniferous forests and its potential implications for the future, *Atmos. Chem. Phys.*, 9, 8079–8090, doi:10.5194/acp-9-8079-2009, 2009. 20007

Boy, M., Petäjä, T., Dal Maso, M., Rannik, Ü., Rinne, J., Aalto, P., Laaksonen, A., Vaattovaara, P., Joutsensaari, J., Hoffmann, T., Warnke, J., Apostolaki, M., Stephanou, E. G., Tsapakis, M., Kouvarakis, A., Pio, C., Carvalho, A., Römpp, A., Moortgat, G., Spirig, C., Guenther, A., Greenberg, J., Ciccioli, P., and Kulmala, M.: Overview of the field measurement campaign in Hyytiälä, August 2001 in the framework of the EU project OSOA, *Atmos. Chem. Phys.*, 4, 657–678, doi:10.5194/acp-4-657-2004, 2004. 20016

Boy, M., Kulmala, M., Ruuskanen, T. M., Pihlatie, M., Reissell, A., Aalto, P. P., Keronen, P., Dal Maso, M., Hellen, H., Hakola, H., Jansson, R., Hanke, M., and Arnold, F.: Sulphuric acid closure and contribution to nucleation mode particle growth, *Atmos. Chem. Phys.*, 5, 863–878, doi:10.5194/acp-5-863-2005, 2005. 20007

Boy, M., Hellmuth, O., Korhonen, H., Nilsson, E. D., ReVelle, D., Turnipseed, A., Arnold, F., and Kulmala, M.: MALTE – model to predict new aerosol formation in the lower troposphere, *Atmos. Chem. Phys.*, 6, 4499–4517, doi:10.5194/acp-6-4499-2006, 2006. 20008, 20009, 20010, 20015

Boy, M., Kazil, J., Lovejoy, E., Guenther, A., and Kulmala, M.: Relevance of ion-induced nucleation of sulfuric acid and water in the lower troposphere over the boreal forest at northern latitudes, *Atmos. Res.*, 90, 151–158, doi:10.1016/j.atmosres.2008.01.002, 2008. 20008

ACPD

10, 20005–20033, 2010

Particle concentration as the indicator of formation mechanism

J. Lauros et al.

Title Page

Abstract

Introduction

Conclusions

References

Tables

Figures

⏪

⏩

◀

▶

Back

Close

Full Screen / Esc

Printer-friendly Version

Interactive Discussion

**Particle
concentration as the
indicator of formation
mechanism**J. Lauros et al.

[Title Page](#)[Abstract](#)[Introduction](#)[Conclusions](#)[References](#)[Tables](#)[Figures](#)[⏪](#)[⏩](#)[◀](#)[▶](#)[Back](#)[Close](#)[Full Screen / Esc](#)[Printer-friendly Version](#)[Interactive Discussion](#)

Boy, M., Sogachev, A., Lauros, J., Zhou, L., Guenther, A., and Smolander, S.: SOSA – a new model to simulate the concentrations of organic vapours and sulphuric acid inside the ABL – Part 1: Model description and initial evaluation, *Atmos. Chem. Phys. Discuss.*, 10, 18607–18633, doi:10.5194/acpd-10-18607-2010, 2010. 20007

5 Damian, V.: The kinetic preprocessor KPP—a software environment for solving chemical kinetics, *Comput. Chem. Eng.*, 26, 1567–1579, doi:10.1016/S0098-1354(02)00128-X, 2002. 20009

Gagné, S., Laakso, L., Petäjä, T., Kerminen, V.-M., and Kulmala, M.: Analysis of one year of Ion-DMPs data from the SMEAR II station, Finland, *Tellus B*, 60, 318–329, doi:10.1111/j.1600-0889.2008.00347.x, 2008. 20008

10 Guenther, A., Karl, T., Harley, P., Wiedinmyer, C., Palmer, P. I., and Geron, C.: Estimates of global terrestrial isoprene emissions using MEGAN (Model of Emissions of Gases and Aerosols from Nature), *Atmos. Chem. Phys.*, 6, 3181–3210, doi:10.5194/acp-6-3181-2006, 2006. 20010

15 Hellmuth, O.: Columnar modelling of nucleation burst evolution in the convective boundary layer – first results from a feasibility study – Part I: Modelling approach, *Atmos. Chem. Phys.*, 6, 4175–4214, doi:10.5194/acp-6-4175-2006, 2006a. 20007

Hellmuth, O.: Columnar modelling of nucleation burst evolution in the convective boundary layer – first results from a feasibility study – Part II: Meteorological characterisation, *Atmos. Chem. Phys.*, 6, 4215–4230, doi:10.5194/acp-6-4215-2006, 2006b. 20007

20 Hellmuth, O.: Columnar modelling of nucleation burst evolution in the convective boundary layer – first results from a feasibility study – Part III: Preliminary results on physicochemical model performance using two “clean air mass” reference scenarios, *Atmos. Chem. Phys.*, 6, 4231–4251, doi:10.5194/acp-6-4231-2006, 2006c. 20007

25 Hellmuth, O.: Columnar modelling of nucleation burst evolution in the convective boundary layer – first results from a feasibility study – Part IV: A compilation of previous observations for valuation of simulation results from a columnar modelling study, *Atmos. Chem. Phys.*, 6, 4253–4274, doi:10.5194/acp-6-4253-2006, 2006d. 20007

Hoppel, W., Frick, G., Fitzgerald, J., and Larsson, R.: Marine boundary layer measurements of new particle formation and the effects nonprecipitating clouds have on aerosol size distributions, *J. Geophys. Res.*, 99, 14443–14459, 1994. 20007

30 Korhonen, H., Lehtinen, K. E. J., and Kulmala, M.: Multicomponent aerosol dynamics model UHMA: model development and validation, *Atmos. Chem. Phys.*, 4, 757–771,

Particle concentration as the indicator of formation mechanism

J. Lauros et al.

[Title Page](#)[Abstract](#)[Introduction](#)[Conclusions](#)[References](#)[Tables](#)[Figures](#)[⏪](#)[⏩](#)[◀](#)[▶](#)[Back](#)[Close](#)[Full Screen / Esc](#)[Printer-friendly Version](#)[Interactive Discussion](#)

doi:10.5194/acp-4-757-2004, 2004. 20010

Kuang, C., McMurry, P., McCormick, A., and Eisele, F.: Dependence of nucleation rates on sulfuric acid vapor concentration in diverse atmospheric locations, *J. Geophys. Res.*, 113, D10209, doi:10.1029/2007JD009253, 2008. 20006

5 Kulmala, M., Hämeri, K. K., Aalto, P., Mäkelä, J., Pirjola, L., Nilsson, E. D., Buzorius, G., Rannik, Ü., Dal Maso, M., Seidl, W., Hoffmann, T., Jansson, R., Hansson, H.-C., O'Dowd, C., and Viisanen, Y.: Overview of the international project on biogenic aerosol formation in the boreal forest (BIOFOR), *Tellus B*, 53, 324–343, 2001. 20008

10 Kulmala, M., Kerminen, V.-M., Anttila, T., Laaksonen, A., and O'Dowd, C. D.: Organic aerosol formation via sulphate cluster activation, *J. Geophys. Res.*, 109, D04205, doi:10.1029/2003JD003961, 2004. 20010

15 Kulmala, M., Lehtinen, K. E. J., and Laaksonen, A.: Cluster activation theory as an explanation of the linear dependence between formation rate of 3 nm particles and sulphuric acid concentration, *Atmos. Chem. Phys.*, 6, 787–793, doi:10.5194/acp-6-787-2006, 2006. 20006, 20007

20 Laakso, L., Anttila, T., Lehtinen, K. E. J., Aalto, P. P., Kulmala, M., Hörrak, U., Paatero, J., Hanke, M., and Arnold, F.: Kinetic nucleation and ions in boreal forest particle formation events, *Atmos. Chem. Phys.*, 4, 2353–2366, doi:10.5194/acp-4-2353-2004, 2004. 20008

25 Laakso, L., Grönholm, T., Kulmala, L., Haapanala, S., Hirsikko, A., Lovejoy, E. R., Kazil, J., Kurtén, T., Boy, M., Nilsson, E. D., Sogachev, A., Riipinen, I., Stratmann, F., and Kulmala, M.: Hot-air balloon as a platform for boundary layer profile measurements during particle formation, *Boreal Environ. Res.*, 12, 279–294, 2007. 20008, 20013, 20016, 20019

30 Lauros, J., Nilsson, E. D., Dal Maso, M., and Kulmala, M.: Contribution of mixing in the ABL to new particle formation based on observations, *Atmos. Chem. Phys.*, 7, 4781–4792, doi:10.5194/acp-7-4781-2007, 2007. 20026

Makkonen, R., Asmi, A., Korhonen, H., Kokkola, H., Järvenoja, S., Räisänen, P., Lehtinen, K. E. J., Laaksonen, A., Kerminen, V.-M., Järvinen, H., Lohmann, U., Bennartz, R., Feichter, J., and Kulmala, M.: Sensitivity of aerosol concentrations and cloud properties to nucleation and secondary organic distribution in ECHAM5-HAM global circulation model, *Atmos. Chem. Phys.*, 9, 1747–1766, doi:10.5194/acp-9-1747-2009, 2009. 20014

Manninen, H. E., Nieminen, T., Riipinen, I., Yli-Juuti, T., Gagné, S., Asmi, E., Aalto, P. P., Petäjä, T., Kerminen, V.-M., and Kulmala, M.: Charged and total particle formation and growth rates during EUCAARI 2007 campaign in Hyytiälä, *Atmos. Chem. Phys.*, 9, 4077–

Particle concentration as the indicator of formation mechanism

J. Lauros et al.

[Title Page](#)[Abstract](#)[Introduction](#)[Conclusions](#)[References](#)[Tables](#)[Figures](#)[⏪](#)[⏩](#)[◀](#)[▶](#)[Back](#)[Close](#)[Full Screen / Esc](#)[Printer-friendly Version](#)[Interactive Discussion](#)

4089, doi:10.5194/acp-9-4077-2009, 2009. 20008

McMurry, P. and Friedlander, S.: New particle formation in the presence of an aerosol, *Atmos. Environ.* (1967), 13, 1635–1651, doi:10.1016/0004-6981(79)90322-6, 1979. 20010

Napari, I., Noppel, M., Vehkamäki, H., and Kulmala, M.: An improved model for ternary nucleation of sulfuric acid-ammonia-water, *J. Chem. Phys.*, 116, 4221–4227, 2002. 20006

Noh, Y., Cheon, W. G., Hong, S.-Y., and Raasch, S.: Improvement of the K-profile model for the planetary boundary layer based on large eddy simulation data, *Bound.-Lay. Meteorol.*, 107, 401–427, 2003. 20007

O'Dowd, C. D., Yoon, Y. J., Junkermann, W., Aalto, P., Kulmala, M., Lihavainen, H., and Viisanen, Y.: Airborne measurements of nucleation mode particles II: boreal forest nucleation events, *Atmos. Chem. Phys.*, 9, 937–944, doi:10.5194/acp-9-937-2009, 2009. 20019

Paasonen, P., Nieminen, T., Asmi, E., Manninen, H. E., Petäjä, T., Plass-Dülmer, C., Flentje, H., Birmili, W., Wiedensohler, A., Hörrak, U., Metzger, A., Hamed, A., Laaksonen, A., Facchini, M. C., Kerminen, V.-M., and Kulmala, M.: On the roles of sulphuric acid and low-volatility organic vapours in the initial steps of atmospheric new particle formation, *Atmos. Chem. Phys. Discuss.*, 10, 11795–11850, doi:10.5194/acpd-10-11795-2010, 2010. 20007

Petroff, A., Mailliat, A., Amielh, M., and Anselmet, F.: Aerosol dry deposition on vegetative canopies – Part 2: A new modelling approach and applications, *Atmos. Environ.*, 42, 3654–3683, doi:10.1016/j.atmosenv.2007.12.060, 2008. 20012, 20013, 20019

Radhakrishnan, K. and Hindmarsh, A. C.: Description and Use of LSODE, the Livermore Solver for Ordinary Differential Equations, Tech. Rep. report UCRL-ID-113855, Lawrence Livermore National Laboratory, 1993. 20010

Rannik, Ü., Aalto, P., Keronen, P., Vesala, T., and Kulmala, M.: Interpretation of aerosol particle fluxes over a pine forest: dry deposition and random errors, *J. Geophys. Res.*, 108, 4544, doi:10.1029/2003JD003542, 2003. 20013

Riipinen, I., Sihto, S.-L., Kulmala, M., Arnold, F., Dal Maso, M., Birmili, W., Saarnio, K., Teinilä, K., Kerminen, V.-M., Laaksonen, A., and Lehtinen, K. E. J.: Connections between atmospheric sulphuric acid and new particle formation during QUEST III–IV campaigns in Heidelberg and Hyytiälä, *Atmos. Chem. Phys.*, 7, 1899–1914, doi:10.5194/acp-7-1899-2007, 2007. 20006

Sandu, A. and Sander, R.: Technical note: Simulating chemical systems in Fortran90 and Matlab with the Kinetic PreProcessor KPP-2.1, *Atmos. Chem. Phys.*, 6, 187–195, doi:10.5194/acp-6-187-2006, 2006. 20009

Particle concentration as the indicator of formation mechanism

J. Lauros et al.

Title Page

Abstract

Introduction

Conclusions

References

Tables

Figures

⏪

⏩

◀

▶

Back

Close

Full Screen / Esc

Printer-friendly Version

Interactive Discussion



Sandu, A., Verwer, J. G., Loon, M. V., Carmichael, G. R., Potra, F. A., Dabdub, D., and Seinfeld, J. H.: Benchmarking stiff ode solvers for atmospheric chemistry problems-I. implicit vs. explicit, *Atmos. Environ.*, 31, 3151–3166, doi:10.1016/S1352-2310(97)00059-9, 1997. 20010

5 Sihto, S.-L., Kulmala, M., Kerminen, V.-M., Dal Maso, M., Petäjä, T., Riipinen, I., Korhonen, H., Arnold, F., Janson, R., Boy, M., Laaksonen, A., and Lehtinen, K. E. J.: Atmospheric sulphuric acid and aerosol formation: implications from atmospheric measurements for nucleation and early growth mechanisms, *Atmos. Chem. Phys.*, 6, 4079–4091, doi:10.5194/acp-6-4079-2006, 2006. 20006

10 Sihto, S.-L., Vuollekoski, H., Leppä, J., Riipinen, I., Kerminen, V.-M., Korhonen, H., Lehtinen, K. E. J., Boy, M., and Kulmala, M.: Aerosol dynamics simulations on the connection of sulphuric acid and new particle formation, *Atmos. Chem. Phys.*, 9, 2933–2947, doi:10.5194/acp-9-2933-2009, 2009 20006

15 Sogachev, A.: A note on two-equation closure modelling of canopy flow, *Bound.-Lay. Meteorol.*, 130, 423–435, 2009. 20009

Sogachev, A. and Panferov, O.: Modification of two-equation models to account for plant drag, *Bound. Lay. Meteorol.*, 121, 229–266, doi:10.1007/s10546-006-9073-5, 2006. 20009

20 Sogachev, A., Menzhulin, G. V., Heimann, M., and Lloyd, J.: A simple three-dimensional canopy – planetary boundary layer simulation model for scalar concentrations and fluxes, *Tellus B*, 54, 784–819, 2002. 20009

Stratmann, F., Siebert, H., Spindler, G., Wehner, B., Althausen, D., Heintzenberg, J., Hellmuth, O., Rinke, R., Schmieder, U., Seidel, C., Tuch, T., Uhrner, U., Wiedensohler, A., Wandinger, U., Wendisch, M., Schell, D., and Stohl, A.: New-particle formation events in a continental boundary layer: first results from the SATURN experiment, *Atmos. Chem. Phys.*, 3, 1445–1459, doi:10.5194/acp-3-1445-2003, 2003. 20016, 20019

25 Stull, R. B.: *An Introduction to Boundary Layer Meteorology*, Kluwer Academic Publishers, Dordrecht, The Netherlands, 670 pp., ISBN: 90-227-2969-4, 1989. 20007

Vehkamäki, H., Kulmala, M., Lehtinen, K., Timmreck, C., Noppel, M., and Laaksonen, A.: An improved parameterization for sulfuric acid–water nucleation rates for tropospheric and stratospheric conditions, *J. Geophys. Res.*, 107, 4622, doi:10.1029/2002JD002184, 2002. 20006

30 Vuollekoski, H., Nieminen, T., Paasonen, P., Sihto, S.-L., Boy, M., Manninen, H., Lehtinen, K. E. J., Kerminen, V.-M., and Kulmala, M.: Atmospheric nucleation and initial steps of particle growth: numerical comparison of different theories and hypotheses, *Atmos. Res.*,

doi:10.1016/j.atmosres.2010.04.007, in press, 2010. 20006, 20007

Weber, R., Marti, J., McMurry, P., Eisele, F., Tanner, D., and Jefferson, A.: Measured atmospheric new particle formation rates: Implications for nucleation mechanisms, Chem. Eng. Commun., 151, 53–64, 1996. 20006

- 5 Weber, R., Marti, J., McMurry, P., Eisele, F., Tanner, D., and Jefferson, A.: Measurements of new particle formation and ultrafine particle growth rates at a clean continental site, J. Geophys. Res., 102, 4375–4385, 1997. 20007

ACPD

10, 20005–20033, 2010

**Particle
concentration as the
indicator of formation
mechanism**

J. Lauros et al.

Title Page

Abstract

Introduction

Conclusions

References

Tables

Figures

⏪

⏩

◀

▶

Back

Close

Full Screen / Esc

Printer-friendly Version

Interactive Discussion



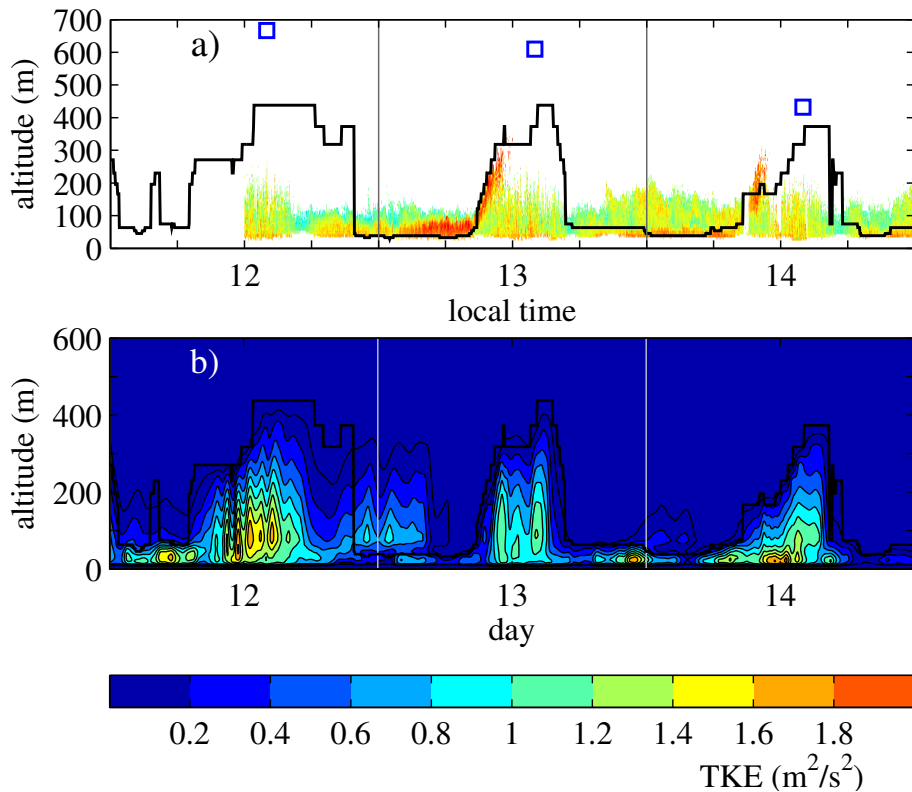


Fig. 1. (a) Mixing height (i) as observed by SODAR, shown by colours, red colour shows the strongest echo and thereby the altitude of temperature inversion, see Lauros et al. (2007), and (ii) as determined from radiosonde measurements in Jokioinen, 100 km to the South from SMEAR II, shown by blue squares, and (iii) as simulated with MALTE, shown by black curve. (b) Turbulence kinetic energy (TKE) from simulations, black curve same as in (a).

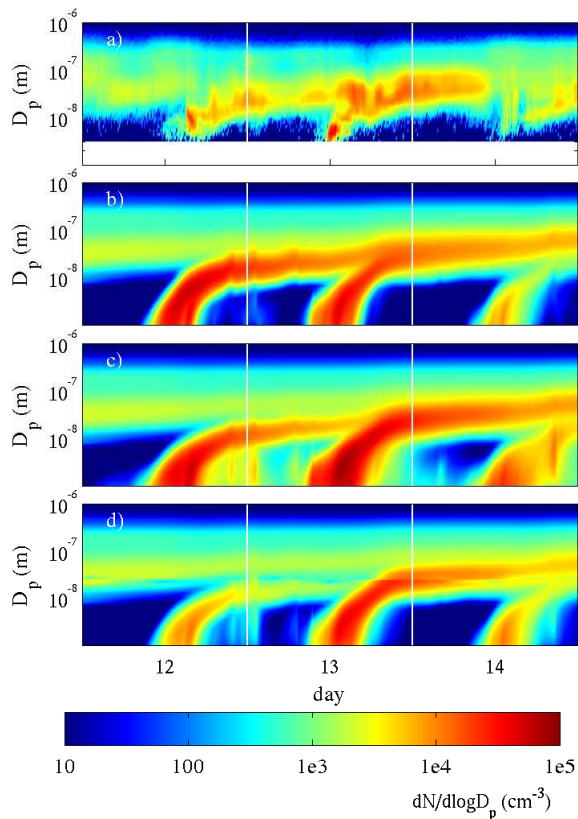


Fig. 2. (a) Observed particle formation events. (b) Typical event simulation for kinetic nucleation (Eq. 1). (c) Typical event when the nucleation rate depends on reaction products of monoterpenes with O_3 (Eq. 2) and (d) typical event when the nucleation rate depends on reaction products of monoterpenes with OH (Eq. 2). In presented simulations the condensing organic vapour participating nano-Köhler growth is composed from reaction products of monoterpenes with OH.

Particle concentration as the indicator of formation mechanism

J. Lauros et al.

Title Page	
Abstract	Introduction
Conclusions	References
Tables	Figures
◀	▶
◀	▶
Back	Close
Full Screen / Esc	
Printer-friendly Version	
Interactive Discussion	



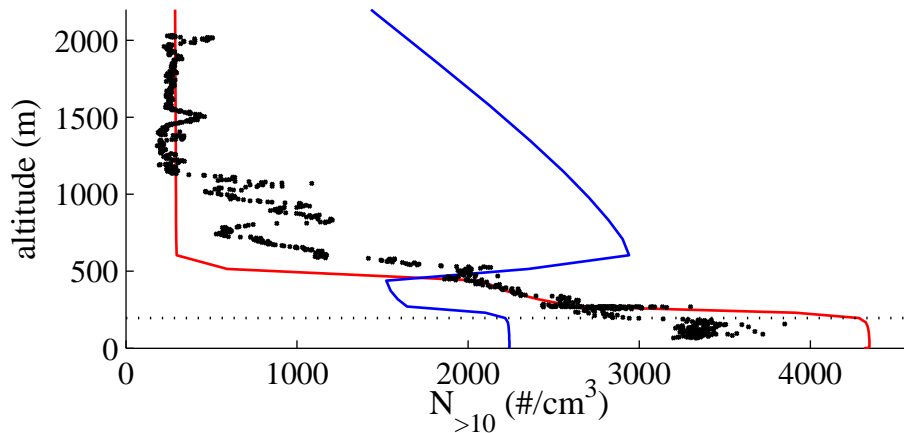


Fig. 3. Observed (black dots) and simulated particle number concentration $N_{>10\text{nm}}$ on 13 March 2006. Organic nucleation (red curve), kinetic nucleation (blue curve) and the ABL height (black dotted line).

Particle concentration as the indicator of formation mechanism

J. Lauros et al.

Title Page	
Abstract	Introduction
Conclusions	References
Tables	Figures
◀	▶
◀	▶
Back	Close
Full Screen / Esc	
Printer-friendly Version	
Interactive Discussion	



Particle concentration as the indicator of formation mechanism

J. Lauros et al.

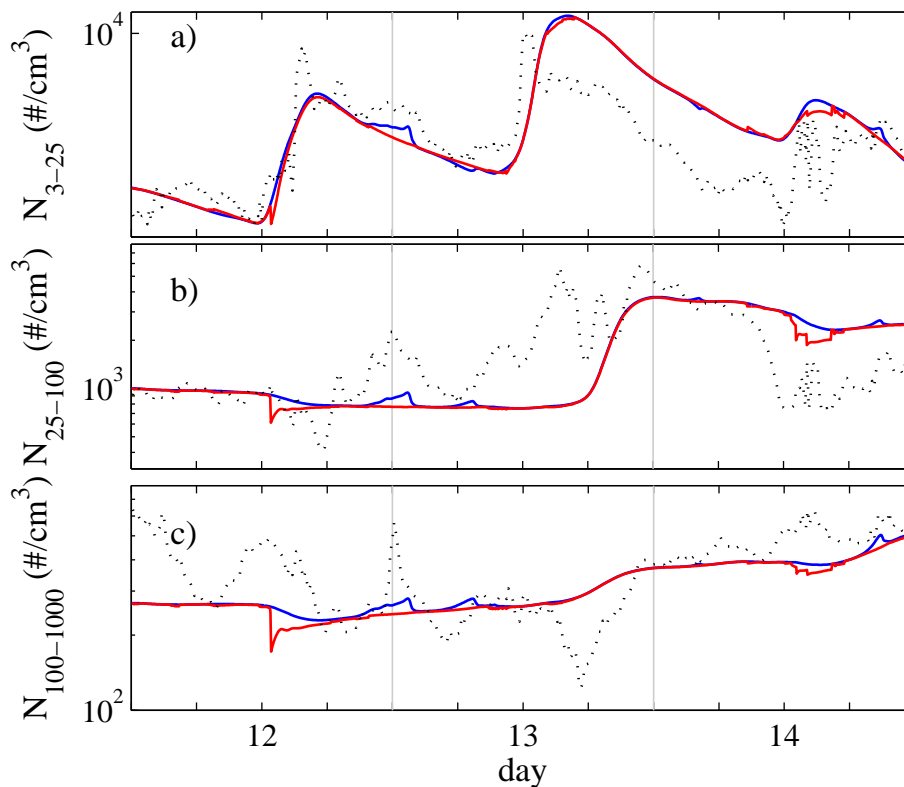


Fig. 4. Simulated particle concentration **(a)** $N_{3-25\text{nm}}$, **(b)** $N_{25-100\text{nm}}$ and **(c)** $N_{100-1000\text{nm}}$ at the top of the ABL (red curve) and at the surface (blue curve). The observed aerosol concentration at the surface is shown by black dotted curve.

Title Page

Abstract

Introduction

Conclusions

References

Tables

Figures

◀

▶

◀

▶

Back

Close

Full Screen / Esc

Printer-friendly Version

Interactive Discussion

Particle concentration as the indicator of formation mechanism

J. Lauros et al.

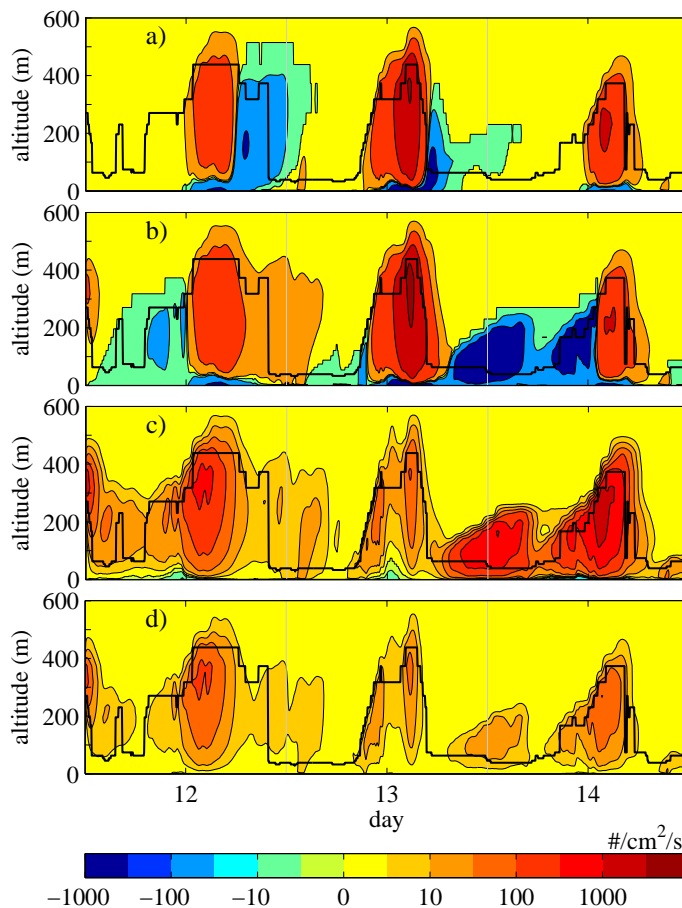


Fig. 5. Turbulent particle flux ($\text{cm}^{-2} \text{s}^{-1}$) for **(a)** 3–6 nm, **(b)** 3–25 nm, **(c)** 25–100 nm and **(d)** 100–1000 nm particles. Black solid curve represents simulated mixing height.

[Title Page](#)[Abstract](#)[Introduction](#)[Conclusions](#)[References](#)[Tables](#)[Figures](#)[◀](#)[▶](#)[◀](#)[▶](#)[Back](#)[Close](#)[Full Screen / Esc](#)[Printer-friendly Version](#)[Interactive Discussion](#)

Particle concentration as the indicator of formation mechanism

J. Lauros et al.

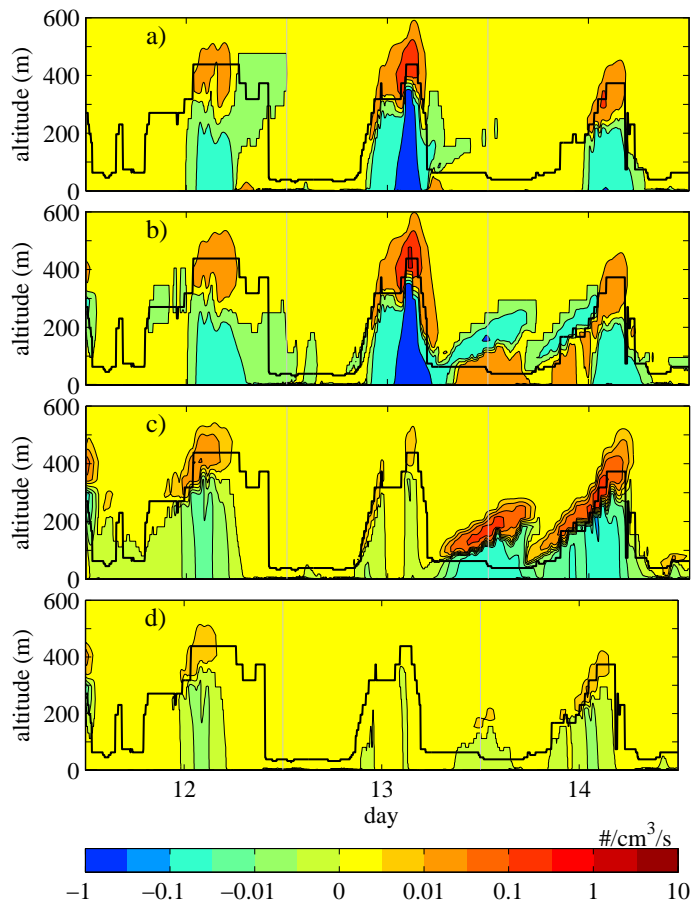


Fig. 6. Effect of turbulent flux on (a) 3–6 nm, (b) 3–25 nm, (c) 25–100 nm and (d) 100–1000 nm particle concentration calculated as $-dF_t/dz$. Black solid curve represents simulated mixing height.

[Title Page](#)[Abstract](#)[Introduction](#)[Conclusions](#)[References](#)[Tables](#)[Figures](#)[◀](#)[▶](#)[◀](#)[▶](#)[Back](#)[Close](#)[Full Screen / Esc](#)[Printer-friendly Version](#)[Interactive Discussion](#)

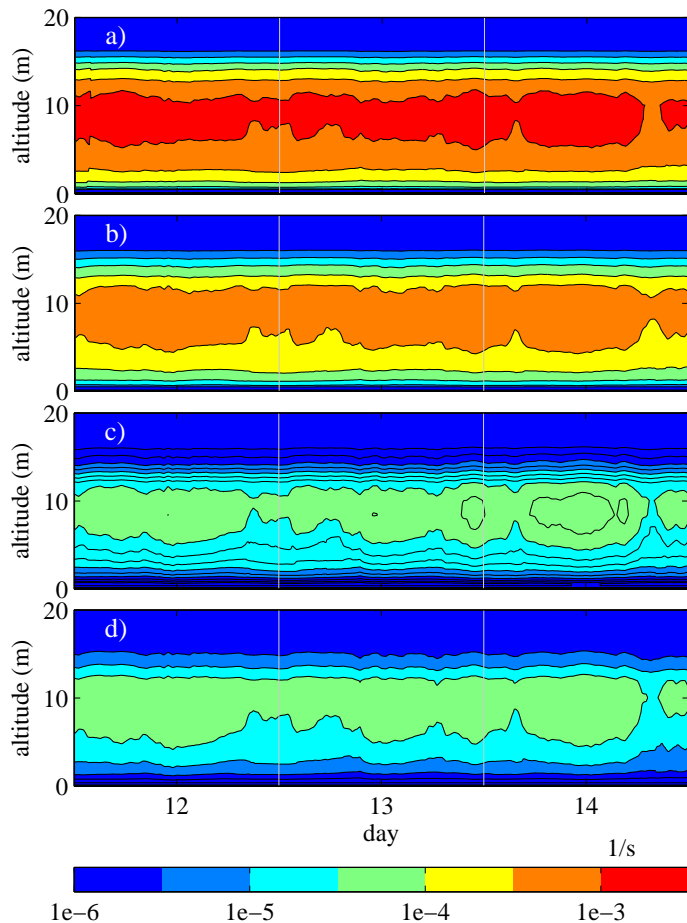


Fig. 7. Median collection rate of **(a)** 3–6 nm, **(b)** 3–25 nm, **(c)** 25–100 nm and **(d)** 100–1000 nm particles. Collection rate is calculated as given by Eq. (3).

Particle concentration as the indicator of formation mechanism

J. Lauros et al.

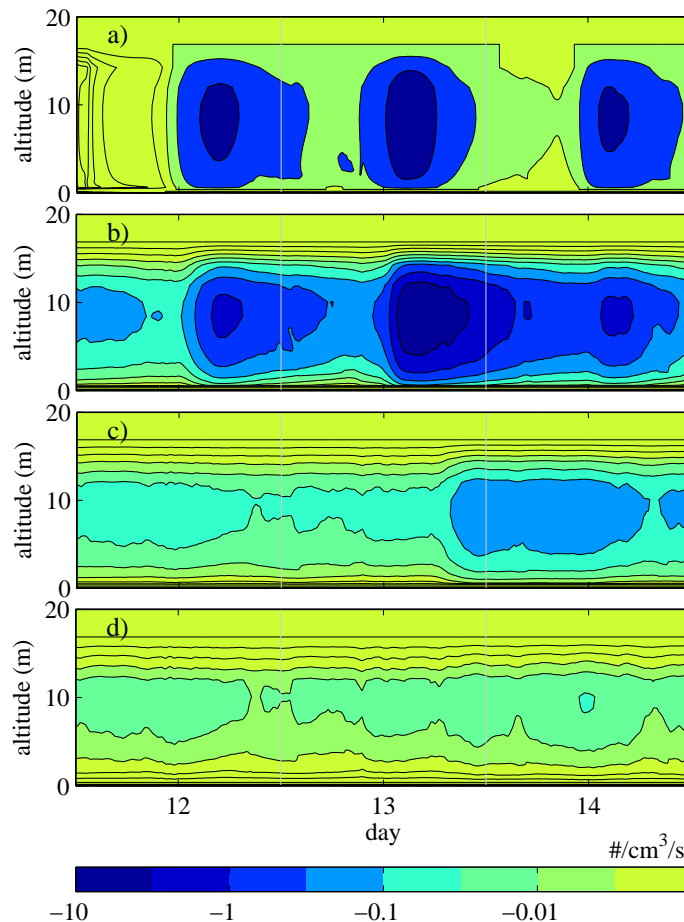


Fig. 8. Removal rate ($\text{cm}^{-3}\text{s}^{-1}$) due to deposition for (a) 3–6 nm, (b) 3–25 nm, (c) 25–100 nm and (d) 100–1000 nm particles. Removal rate is calculated as given by Eq. (4).

[Title Page](#)[Abstract](#)[Introduction](#)[Conclusions](#)[References](#)[Tables](#)[Figures](#)[◀](#)[▶](#)[◀](#)[▶](#)[Back](#)[Close](#)[Full Screen / Esc](#)[Printer-friendly Version](#)[Interactive Discussion](#)